

## A Comparison of ERBE and AVHRR Longwave Flux Estimates

Sung Nam Oh

Systems Engineering Research Institute  
Korea Institute of Science and Technology

(Received September 1, 1990 ; Accepted September 10, 1990)

### ERBE와 AVHRR에 의하여 추정된 지구의 장파복사량 비교

오 성 남

한국과학기술연구원 시스템공학센터  
(1990년 9월 1일 받음; 1990년 9월 10일 수리)

#### 요 약

NOAA 위성의 narrow-band AVHRR(Advanced Very High Resolution Radiometer) 적외선 채널과 broad-band  $0.2\sim 50\mu\text{m}$  영역의 ERBE(Earth Radiation Budget Experiment) scanning instruments에 의하여 관측된 radiance로부터 추정된 지구의 대기 외 장파복사량(Outgoing Longwave Radiation:OLR)이 비교조사되었다. 이를 위하여 1985년 4월, 7월, 10월과 1986년 1월에 위성에서 관측된 radiance를 각각 이용하였고 비교된 OLR은 위도와 경도가 각각  $2.5^\circ$ 간격으로 구분된 grid 내에서 일치(collocate)시켜 지역별(zonal), 그리고 전지구(global) 규모로 비교되었다.

ERBE와 AVHRR에 의하여 각각 추정된 OLR값의 차(ERBE minus AVHRR)에 의한 분석 결과는 주간(주간)의 경우  $-1\sim 2\text{ W/m}^2$ 의 값과 야간의 경우  $4\sim 7\text{ W/m}^2$ 의 값으로 비교적 좋은 일치를 보였지만 이들의 RMS는 하절(6월)에  $12\text{ W/m}^2$ 와 동절(12월)에  $5\text{ W/m}^2$ 의 값으로 다소 높은 차이를 보였다. 한편, 이들 OLR 값은 관측지역에 따라 큰 차이를 나타내어 사막지역과 아열대고기압(subtropical ocean)대에서는 상반된 결과를 보였다.

이들 지역에 대한 차이는 지역적 기온구조와 지표온도의 영향을 다 고려하지 못하고 OLR 측정치를 도출하는 대기복사모델(radiation model)의 regional systematic bias에서 기인된 것으로 해석된다. 즉 사막의 지표역전층에 대한 AVHRR과 해면의 대기구조에 대한 ERBE의 OLR은 상반된 영향을 보였다.

## 1. Introduction

The outgoing longwave radiation(OLR) has been obtained by NOAA polarorbiting satellite observations from the 10-12 $\mu\text{m}$  window region beginning in June, 1974(Gruber and Winston, 1978). New algorithms were developed in subsequent years to improve the accuracy of the OLR(Gruber and Kruger, 1984). With the NOAA and TIROS series of satellites, a continuous orbital presence has been maintained with both morning and afternoon sun-synchronous satellites carrying initially the Scanning Radiometer(SR) and later the Advanced Very High Resolution Radiometer(AVHRR) instruments. Narrow-band to broad-band spectral corrections have been developed(Ohring et al., 1984) and applied to the OLR data to estimate the spectrally integrated longwave flux leaving the Top of Atmosphere(TOA). The data have been widely utilized in many weather climate diagnostic studies(e.g., Lau and Chen, 1983; Liebmann and Hartman, 1982). However, it has only been since the Earth Radiation Budget Experiments (ERBE)(Barkstrom et al., 1988) that we have been able to obtain coincident and simultaneous comparisons between the NOAA estimates of OLR and broadband flux estimates as produced by ERBE. Such comparisons are important since it allows for an assesment of the accuracy of the OLR data which in turn impacts its use and plans for continued production of the data.

The objective of this study is to compare ERBE and NOAA OLR data sets in two ways. One is to examine data that are collocated in time and space(within some specific window), the other to utilize mapped products generally provided to the user community. From here on it will be designated the NOAA estimates of OLR as AVHRR and ERBE estimates as ERBE.

## 2. Data

The OLR data is obtained from the 11.5~12.5 $\mu\text{m}$  window channel of AVHRR flown on the NOAA 9 satellite. NOAA 9 also carried an ERBE narrow field of view instrument. The ERBE scanner has 3 channels : a shortwave(0.2~5 $\mu\text{m}$ ), a longwave(5~50 $\mu\text{m}$ ) and a total channel(0.2~50 $\mu\text{m}$ ). Both are cross track scanners with the AVHRR having an effective footprint of about 4km at nadir and the ERBE about 50km. The nominal equator crossing time is 0230 and 1430 local times. Both sets of data are processed to a 2.5 $\times$ 2.5 degree latitude/longitude grid. The ERBE grid is offset from the AVHRR grid by 1.25 $^\circ$  in latitude and longitude. The

AVHRR data were converted to the ERBE grid by averaging over the four surrounding grid points. Comparisons were performed for April, July, October 1985, and January 1986. In collecting a compatible space and time data set care was taken to insure that both ERBE and AVHRR data were present for a particular grid and time. If one of the grid boxes had missing data the other was not used. This can result in less than a full sample of days, as shown in Fig. 1 for a grid located at 8.75°N, 18.75°E for April 1985.

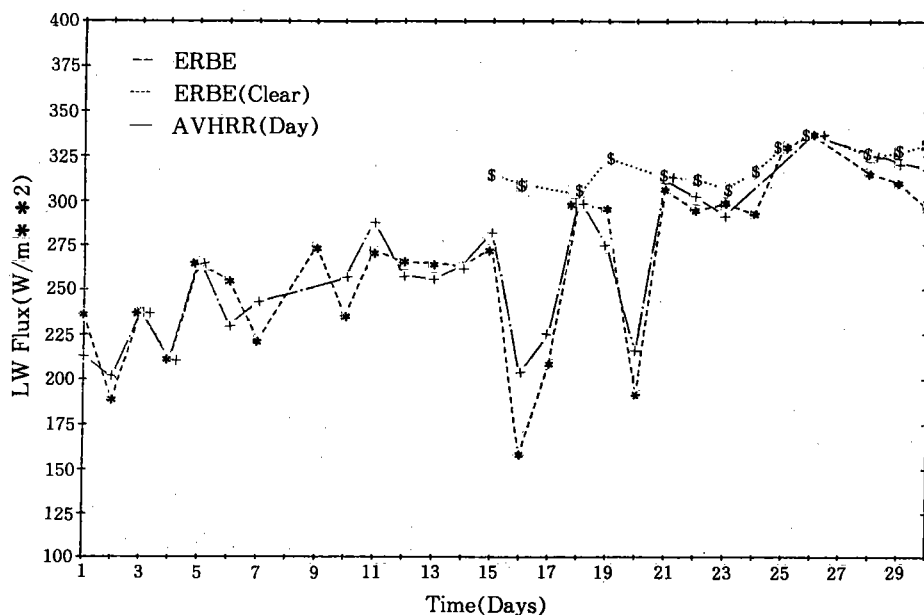


Fig. 1. Time series of ERBE and NOAA OLR (Africa, April 1985).

For this region, 24 matches were obtained; as frequently as once per day and as infrequently as once in 6 days. This figure also illustrates some of the characteristics of the two data sets. For example, the day to day variability, due primarily to convective cloud changes, is observed by both instruments. The ERBE fluxes do appear to have slightly greater sensitivity than the NOAA flux estimates. This may, in part, be attributed to the fact that a regression model, which is inherently less sensitive than reality, are used to transform AVHRR window channel to broad band and flux.

However, as we will show later, there are other factors, such as a lack of sensitivity of the

window channel to particular atmospheric moisture and temperature profiles, that play an important role in the distribution of errors.

### 3. Data Analysis

In this section we will start with comparison on the global scale proceed to the zonal average scale and conclude with comparisons of the regional differences as depicted on analyzed maps.

#### 3.1 Global Scale

The global comparison is shown in Fig. 2, which shows the mean(ERBE-NOAA) and RMS difference between the 2 data sets. Results are shown for both day and night. The RMS difference is about  $12\sim 14\text{ Wm}^{-2}$  while the mean difference varies between about  $-1$  to  $1\text{ Wm}^{-2}$  during the daytime but is about  $5\sim 7\text{ Wm}^{-2}$  during the nighttime. Interestingly this difference between the day and night might be related to a bias noted in the ERBE scanner flown on NOAA-9 which tends to yield a longwave flux during the daytime that is about 2% too low (Green, personal communication, 1989). This apparently comes about because, during the daytime the longwave flux is obtained as the difference between the total and shortwave channel, and during the night only the total channel is used. The shortwave channel is apparently too high,

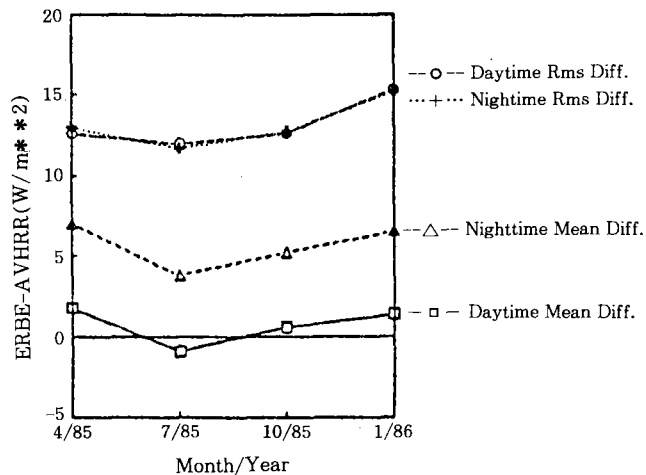


Fig. 2. Global mean difference ERBE-NOAA and RMS difference.

resulting in longwave flux estimates that are low during the daytime for ERBE. However, as will be seen when we discuss the regional comparisons, a significant cause of the differences between ERBE and AVHRR estimates of outgoing longwave radiation are probably related to problems associated with the inability of a window channel to adequately detect significant departures of the atmospheric moisture and temperature profiles from the average.

The linear correlation of the two data sets varies from .95 to .97, indicating a high degree of spatial agreement between the two data sets.

### 3.2 Zonal Scale

The zonal average profile of ERBE and NOAA OLR from 90°N to 90°S for July, 1985 is shown in Fig. 3 for nighttime and Fig. 4 for daytime. Only July will be shown as the other months exhibit similar behavior.

As shown in Fig. 3 the general agreement is quite good in terms of the large-scale structure (e. g., the equator-to-pole gradient, the location and intensity of the ITCZ), but systematic differences are evident between the two data sets at all latitudes. During the day, Fig. 4, the general offset between the two data sets is reduced, and the bias that had been evident over the

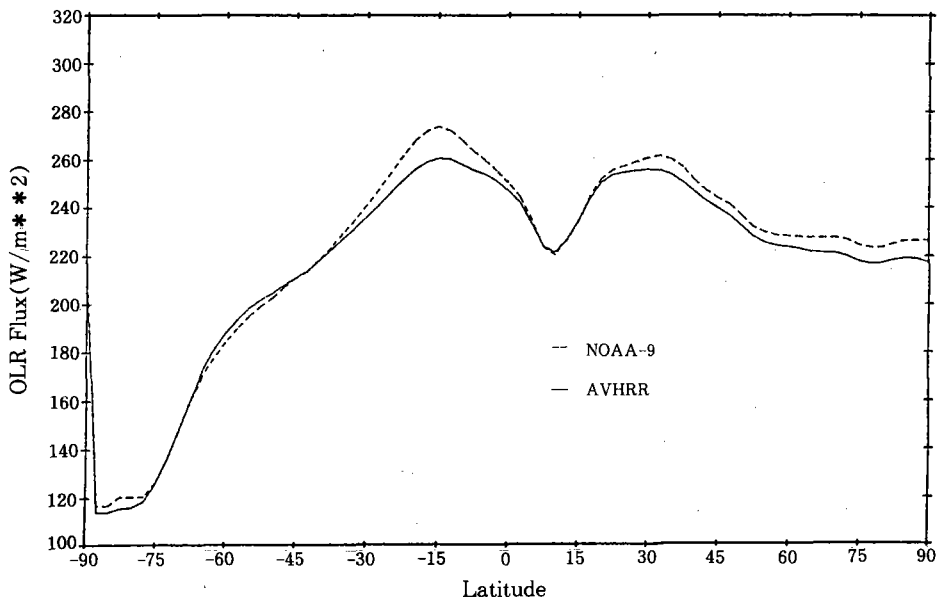


Fig. 3. Zonal profile of ERBE(NOAA 9) and AVHRR OLR for July, 1985 nighttime.

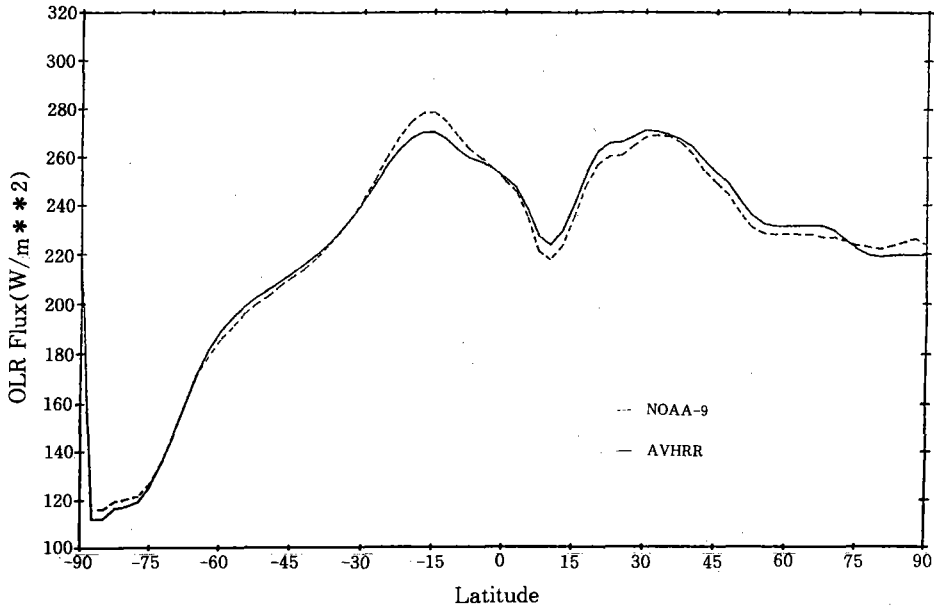


Fig. 4. Same as Fig. 3, but for daytime.

subtropical belt of the summer hemisphere has vanished, although there are still systematic differences in the N. H. subtropics and the polar latitudes. This behavior is consistent with that noted earlier in the global differences.

### 3.3 Regional Comparisons

The daytime emitted TOA longwave flux field for July 1985 as estimated by ERBE is illustrated in Fig. 5. Low OLR values are encountered at the high latitudes, and particularly over Antarctica where they drop below  $100 \text{ Wm}^{-2}$  due to the low winter surface temperatures. The highest OLR, which can exceed  $340 \text{ Wm}^{-2}$ , is encountered over the subtropical belts near  $30^\circ\text{N}$  and  $20^\circ\text{S}$ , where warm surface temperatures combine with a dry, clear, and relatively transparent atmosphere. While the structure of the field at high latitudes is primarily zonal and driven by the latitudinal temperature gradient, more east-west variability is present in the tropics and mid-latitudes. The convective areas over central Africa, the Indian monsoon, and the eastern Pacific Ocean ITCZ show up clearly, as do the oceanic subtropical highs and the continental deserts. The corresponding longwave flux field as estimated by AVHRR is provided in Fig. 6.

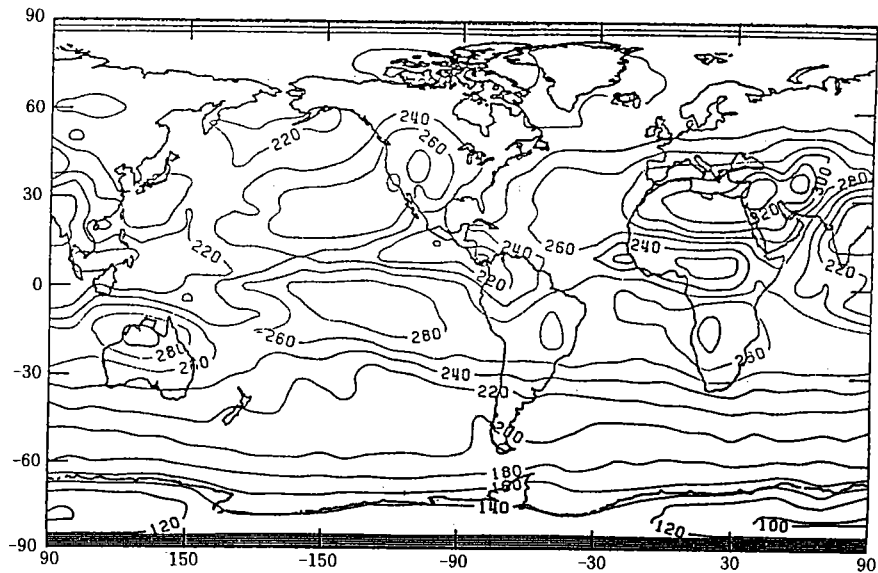


Fig. 5. Daytime OLR distributions(mean value) for ERBE analysis in July, 1985.

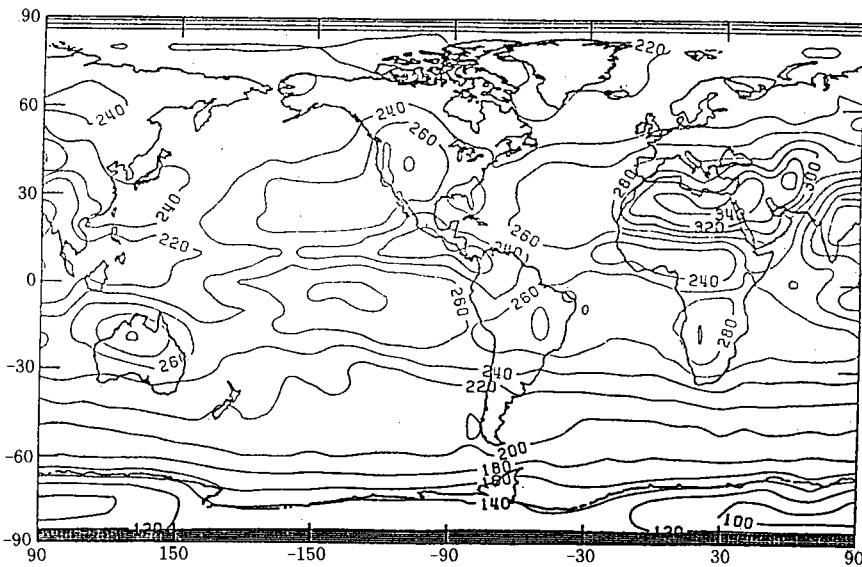


Fig. 6. Daytime OLR distributions(mean value) for AVHRR estimation in July, 1985.

Though subtle differences are apparent, all of the salient features of the ERBE field are well replicated in pattern and magnitude.

The difference between the two daytime OLR estimates(ERBE minus AVHRR) is presented in Fig. 7. The dominant feature of this map is the set of systematic biases of from 5 to 15  $\text{Wm}^{-2}$  present over the oceanic subtropics, where the AVHRR measurements are consistently lower than the ERBE values. A second feature worthy of note is the area of pronounced negative difference(exceeding  $-15 \text{ Wm}^{-2}$ ) over the Sahara desert and northern Africa Saudi Arabia in general, where the AVHRR estimates exceed those from ERBE. Poleward of the  $30^\circ$  latitudes, the agreement between the AVHRR longwave flux estimates is generally good for this month.

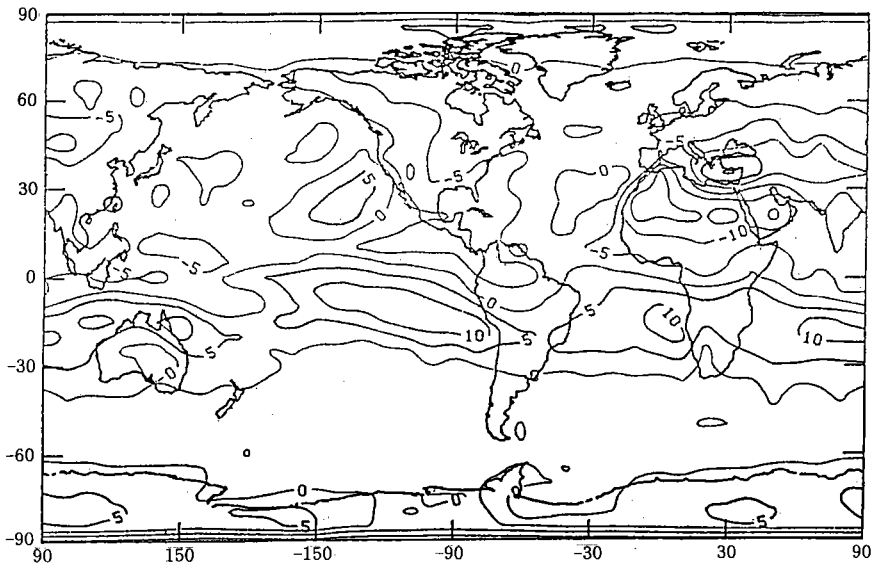


Fig. 7. Daytime mean OLR differences(ERBE-AVHRR) in July, 1985.

The difference between the AVHRR and ERBE OLR fields at night is portrayed in Fig. 8. The nighttime differences are quite similar to those of the daytime with two notable departures. First, the differences between the two estimates are on the order of  $5 \text{ Wm}^{-2}$  greater at night than during the day; this is particularly evident over the oceans. Second, the negative difference over north Africa, and a smaller region over Australia, have vanished. Now, difference maxima are present over Africa and Australia.



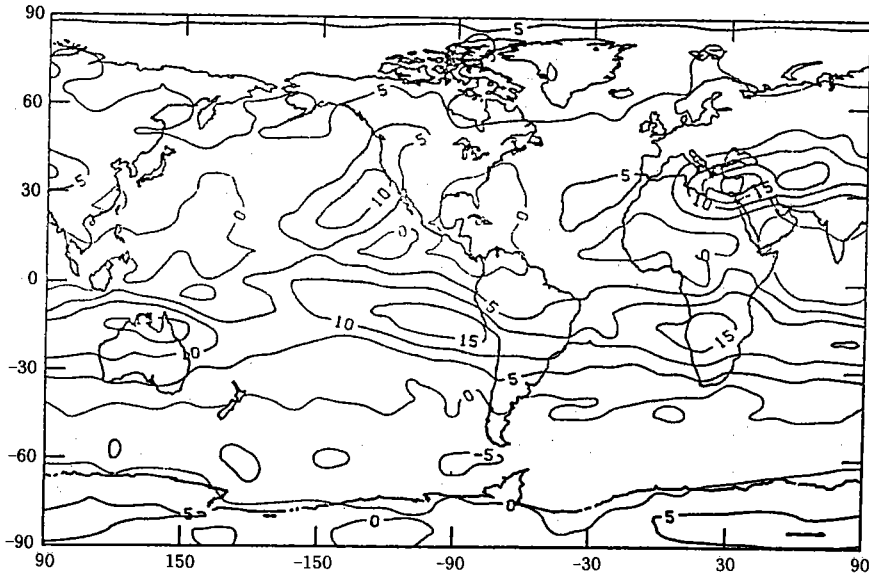


Fig. 8. Same as Fig. 7 but for nighttime.

#### 4. Discussion

Though it has been found that the AVHRR and ERBE estimates of the longwave flux fields bear excellent resemblance in space and time, the observational results presented in the previous section have led to the identification of regional systematic differences between the two sets of measurements. The most dramatic differences were found over the oceanic subtropical high-pressure regions ( $ERBE > AVHRR$ ), and the daytime deserts ( $AVHRR > ERBE$ ). Because these regions have persistent climatological features we suspect that the differences are in large part driven by an inability of the AVHRR algorithm to deal with the atmospheric structure found in those areas.

The temperature and moisture structure in sub-tropical high pressure zones is characterized by a "trade wind" inversion (Riehl, 1979) which is strongest in the eastern ocean and weakens as one progresses westward. Desert areas experience enormous diurnal changes of soil surface temperature which can lead to corresponding large soil surface-air temperature discontinuities. Smith (1986) reports 2.5 cm soil-air temperature discontinuities of about  $25 \sim 30^\circ\text{C}$  during the day and near zero or  $\pm$  a few degrees centigrade temperature discontinuity at night over a sta-

tion in the Arabian Peninsula. Stowe, et al(1988), found similar results over deserts comparing skin temperature from a 10~12  $\mu\text{m}$  radiometer and analyzed surface air temperatures. Since these regions are mostly cloud free or have few clouds the single channel AVHRR algorithm may be insensitive to the variations in atmospheric moisture and temperature structure and return fluxes that are highly related to the surface temperature. Relative to a broad-band flux determination such as available from ERBE, one might expect the AVHRR to overestimate flux values over deserts during the day, be similar in magnitude to deserts during the night and underestimate the flux over the trade wind region in proportion to the strength of the inversion and moisture distribution. Interestingly, the magnitude of the ERBE-AVHRR differences over the oceans decreases as one moves westward consistent with the observed weakening of the trade wind inversion and increase in moisture.

These ideas were tested by calculating the sensitivity of the operational single-channel algorithm to variations of temperature structure and temperature and water vapor trade-wind inversion. Each will be described below.

#### 4.1 Desert Areas

For the desert areas a set of observed atmospheric soundings (pressure, temperature, and dewpoint depression) were collected from various desert locations (Texas, Egypt, Algeria and Nigeria). The soundings were separated into daytime and nighttime, and longwave fluxes were calculated using an updated version (Ellingson et al., 1989a), of the model of Ellingson and Gille (1978), and comparisons were made to OLR estimated from AVHRR 11  $\mu\text{m}$  channel. The calculated broad-band OLR was taken as "truth." Calculations were based on the soundings as given and for various temperature discontinuities between the surface skin temperature and air temperature. For the day (night) soundings temperature discontinuities of +1(-1), +3(-3), +5(-5), +10(-10), +15(-15), and +20(-20)°C were tested.

The results of the calculations are shown in Fig. 9. The variation is nearly linear over the range of temperature calculated, with a slightly different slope during nighttime hours. The important to note is that the magnitudes of the differences are consistent with the observed differences between ERBE and AVHRR and is also supported by the skin-air temperature differences reported by Smith(1986) and Stowe et al.(1988).

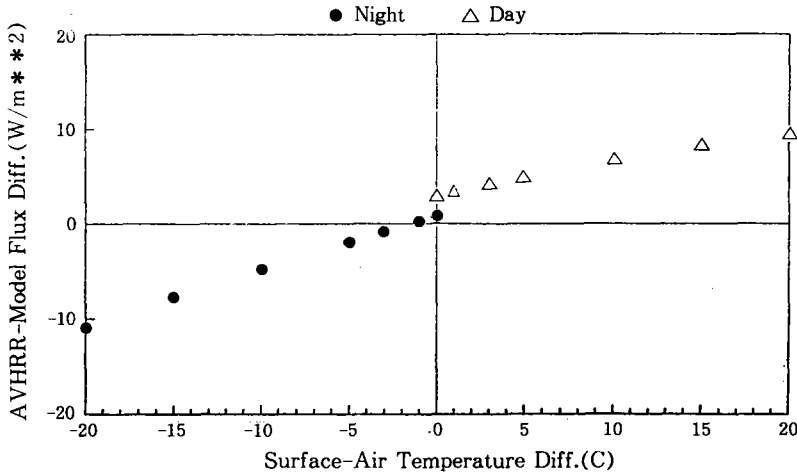


Fig. 9. Skin-Air OLR flux differences of day and night from desert simulations.

#### 4.2 Trade-Wind Region

The calculations for the trade wind region were performed for a typical trade wind sounding taken from Riehl(1954). The strength of the inversion was modified from  $+2$  to  $-10^{\circ}\text{C}$  increments. The water content was held fixed. The results are summarized in Fig. 10. The results show AVHRR estimated flux less modeled flux by  $14\text{ Wm}^{-2}$  to about  $-8\text{ Wm}^{-2}$  depending on inversion strength.

A simulation was also performed to test the sensitivity of the calculations to variations in water vapor, which increase from east to west along the trade wind inversion. For an increase of precipitable water from about 2 to 3 cm(Riehl, 1954), we expect the difference between AVHRR and ERBE to decrease by about  $5\text{ Wm}^{-2}$  mainly due to a decrease in ERBE flux with hardly any decrease in AVHRR.

Thus, not only will the weakening trade-wind inversion lead to smaller differences between AVHRR and ERBE, but so will the variation of water vapor. The results of both temperature and moisture simulations support the view that the cause of the systematic error observed in the tropical oceans is the inability of the window channel algorithm to respond to the unique and persistent temperature and moisture structure present in the trade-wind region.

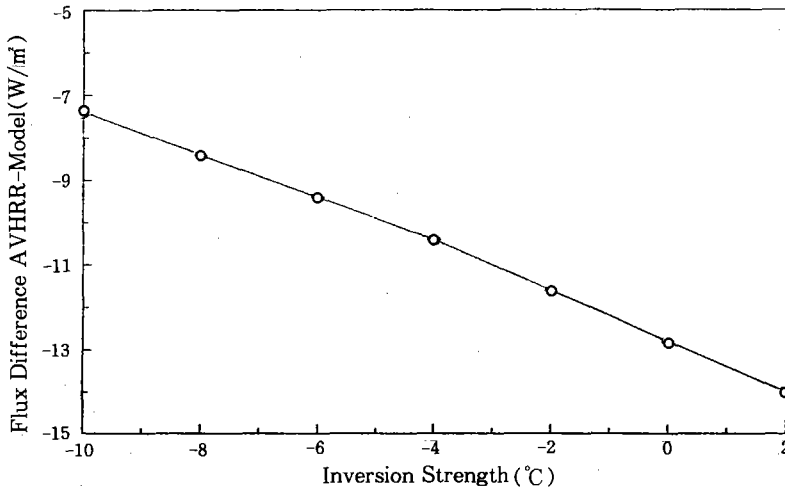


Fig. 10. Flux differences vs inversion strength from trade wind simulations.

## 5. Conclusions

Comparisons were made between narrow-band AVHRR and broad-band ERBE estimates of the OLR at the TOA using both collocated and coincident estimates and monthly averaged estimates (with time and space averaging included) at a  $2.5^\circ$  spatial resolution. In general, the two data sets were found to be in good agreement, with the fundamental variability in time and space, as well as the mean state, well portrayed by either set of measurements. However, systematic biases are observed between the two data sets, particularly over the subtropical oceans, the daytime deserts. This suggests limitations in the applicability of the narrow-band to broad-band spectral correction. This was confirmed by simulations for observed temperature and moisture structures in those regions. The single channel AVHRR is too insensitive to properly depict the unique and persistent climatological features found in those regions. Further improvements in the consistency of narrow-band OLR estimates may be possible through the use of additional information available from multiple spectral channels (e.g., 1989b) or through the use of correction algorithms that are region or air mass-dependent (Jacobowitz, Gruber, and Hucek, 1990).

## 감 사

본 연구는 미국해양기상청(National Oceanic and Atmospheric Administration)의 후원으로 The University of Maryland 기상학과와 기후연구센터(Cooperative Institute for Climate Studies)와의 공동연구 결과이다. 연구를 지도하며 도와 주신 Dr. Robert Ellingson 교수와 NOAA의 Dr. Arnold Gruber 부장에게 감사하고 컴퓨터 계산을 도와준 메릴랜드 기상학과 Mr. 李海天 학생에게 감사한다.

## References

- Barkstrom, B. R., E. F. Harrison, G. L. Smith and R. D. Cess, the ERBE science team, and the ERBE data management team, 1988 : Earth radiation budget experiment(ERBE) validation, archival, and april 1985 results, *Bull. Amer. Meteor. Soc.*, In Press.
- Ellingson, R. E. and J. C. Gille, 1978 : An infrared radiative transfer model. Part 1 : Model description and comparison of observations with calculations, *J. Atmos. Sci.*, **35**, 523~545.
- \_\_\_\_\_, D. J. Yanuck and A. Gruber, 1989a : On the effects of the choice of meteorological data on radiation model simulation of the NOAA technique for estimation outgoing longwave radiation from satellite radiance observations, *J. Clim.*, **2**, 761~765.
- \_\_\_\_\_, \_\_\_\_\_, H. T. Lee and A. Gruber, 1989b : A technique for estimating outgoing longwave radiation from HIRS radiance observations, *J. Ocean. Atmos. Techn.*, **6**, 706~711.
- Gruber, A., and A. F. Kruger. 1984 : The status of the NOAA outgoing longwave radiation data set, *Bull. Am. Meteorol. Soc.*, **65**, 958~962.
- \_\_\_\_\_ and J. S. Winston, 1978 : Earth atmosphere radiative heating based on NOAA scanning radiometer measurements, *Bull. Am. Meteorol. Soc.*, **59**, 1570~1573.
- Jacobowitz, H., A. Gruber and Hucek, 1990 : Preprint, 7th AMS Conference on atmospheric radiation, July 23~27, 1990, San Francisco, CA.
- Lau, K. M. and P. H. Chan, 1983 : Short-term climate variability and atmospheric teleconnections from satellite-observed outgoing longwave radiation. Part 1 : Simultaneous relationship, *J. Atmos. Sci.*, **40**, 2735~2750.

- Liebmann, B. and D. L. Hartmann, 1982 : Interannual variation of outgoing IR associated with tropical circulation change during 1974~1978, *J. Atmos. Sci.*, **39**, 1153~1162.
- Ohring and Gruber, 1983 : Satellite radiation observations and climate theory, *Advances in Geophysics*, **25**, 237~304.
- Riehl, H., 1954 : *Tropical meteorology*. McGraw-Hill, New York, 392
- \_\_\_\_\_, 1979 : *Climate and weather in the tropics*, Academic Press, 611.
- Smith, E. A., 1986 : The structure of the Arabian heat low. Part I : Surface energy budget, *Mo. Wea. Rev.*, **114**, 1067~1083.
- Stowe, L. L., C. G. Wellemeier, T. F. Eck, H.Y.M. Yeh and the Nimbus-7 Cloud Date Processing Team, 1988 : Nimbus-7 global cloud climatology. Part I : Algorithms and validation, *J. Clim.* **1**, 445~470.